Adsorption of ammonia on multilayer iron phthalocyanine.

Isvoranu, Cristina; Knudsen, Jan; Ataman, Evren; Schulte, Karina; Wang, Bin; Bocquet, Marie-Laure; Andersen, Jesper N; Schnadt, Joachim

Published in:
Journal of Chemical Physics

DOI:
10.1063/1.3563636

2011

Adsorption of ammonia on multilayer iron phthalocyanine

Cristina Isvoranu,[1] Jan Knudsen,[1] Evren Ataman,[1] Karina Schulte,[2] Bin Wang,[3] Marie-Laure Bocquet,[3] Jesper N. Andersen,[1] and Joachim Schnadt[1]
[1]*Division of Synchrotron Radiation Research, Department of Physics, Lund University, Box 118, 221 00 Lund, Sweden*
[2]*MAX-lab, Lund University, Box 118, 221 00 Lund, Sweden*
[3]*Laboratoire de chimie, Ecole normale supérieure de Lyon, 46, Allée d'Italie, 69364 Lyon Cedex 07, France*

(Received 15 October 2010; accepted 18 February 2011; published online 21 March 2011)

The adsorption of ammonia on multilayers of well-ordered, flat-lying iron phthalocyanine (FePc) molecules on a Au(111) support was investigated by x-ray photoelectron spectroscopy. We find that the electron-donating ammonia molecules coordinate to the metal centers of iron phthlalocyanine. The coordination of ammonia induces changes of the electronic structure of the iron phthalocyanine layer, which, in particular, lead to a modification of the FePc valence electron spin. © *2011 American Institute of Physics*. [doi:10.1063/1.3563636]

I. INTRODUCTION

Phthalocyanines, as shown in Fig. 1, are planar aromatic compounds, which consist of four isoindole units linked together by nitrogen atoms and which are characterized by an electron cloud delocalized over the alternating carbon and nitrogen atoms.[1] In its center, the phthalocyanine molecule may hold an ion from a large variety of different metal elements and the compound is then termed a metal phthalocyanine.[2] From a technological point-of-view, metal phthalocyanines have been considered for applications in organic light-emitting diodes,[3–5] organic thin film transistors,[6,7] solar cells,[7,8] gas sensors,[9–17] and catalytic applications.[18–21] Of fundamental importance to all these applications is the electronic structure of the various metal phthalocyanine compounds, which conveys highly interesting optical, chemical, and physical properties to the molecules. More specifically, the iron phthalocyanine (FePc) compound has an open valence *d* shell, which results in a number of energetically close-lying electronic states. Their energy distribution can be modified in a number of ways, e.g., by attachment of side groups to the phthaloycanine macrocycle,[22] single-molecule manipulation,[23] change of support,[24] exchange of the metal center[25–28] or, as pursued here, by adsorption of molecular ligands. Specific ligands can be used to tailor the electronic properties of the compound, which also implies that the spin state and thus the magnetic properties of the phthalocyanine can be controlled.

The present study focuses on the influence of adsorption of ammonia (NH_3) on the spin state of the FePc molecule. Using x-ray photoelectron spectroscopy we show that the formation of a dative bond between ammonia and the phthalocyanine iron center leads to a quenching of the spin, which we interpret in terms of a reorganization of the electronic state upon ammonia adsorption. The experimental results are supported by density functional theory (DFT) calculations of the spin magnetic moment, which is shown to drop from $\sim 2\ \mu_B$ for the free molecule to less than $0.3\ \mu_B$.

II. METHODS

The experimental work was carried out at the spectroscopy end station of beam line I311 (Ref. 29) of the Swedish national synchrotron radiation facility MAX-lab in Lund. The end station with separate preparation and analysis chambers is equipped with a SCIENTA SES200 electron energy analyzer. The base pressure in the preparation chamber is in the high 10^{-11} mbar and in the analysis chamber in the mid 10^{-11} mbar range. The Au(111) single crystal was cleaned by repeated cycles of argon ion sputtering (energy 1 keV) and annealing. For annealing a current was passed through the tungsten wire, with which the crystal was mounted to the helium cryostat until the temperature reached 770 K. The sample was kept at this temperature for 10 min. The FePc molecules, purchased from Sigma-Aldrich with a purity of 90%, were thoroughly degassed for several days at temperatures slightly lower than the evaporation temperature. Before sublimation from a resistively heated tantalum pocket the powder was further degassed by heating to the evaporation temperature of 650 to 670 K for approximately 3–4 h. During sublimation the Au(111) substrate was kept at room temperature. After multilayer deposition, the sample was cooled down to ~20 K using liquid helium. The ammonia was dosed through the gas delivery system of the preparation chamber to the sample held at 20 K. The dose is specified in Langmuirs ($1\ \text{L} = 10^{-6}$ torr $\times$ s).

The N 1*s* XAS experiments were performed in Auger yield mode using the linearly polarized synchrotron light of beam line I311. Several light incidence angles were considered: 0°, 20°, 40°, 55°, and 70° incidence with respect to the surface normal. The photon energy scale was calibrated by recording Au 4*f* photoemission spectra excited by first and second order light at relevant photon energies. The intensity of the x-ray absorption spectra was beam line transmission-corrected by dividing the spectra by the energy-dependent photon flux, which was recorded by measuring the photoinduced current on a photodiode placed between the

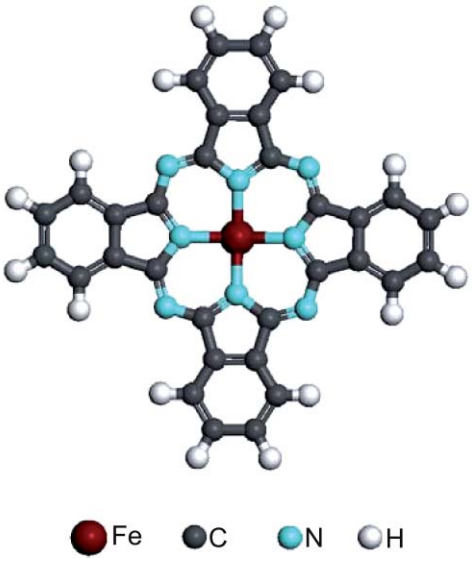

FIG. 1. Molecular structure of iron phthalocyanine.

monochromator and sample. Further, a constant background determined at the low-energy side of the spectra was subtracted and the spectra were then normalized to the height of the step edge determined at around 25 eV above the adsorption edge.[30]

All x-ray photoelectron experiments were carried out in normal emission geometry. The C 1*s*, N 1*s*, and Fe 2*p* x-ray photoelectron spectra were recorded using photon energies of 385, 525, and 820 eV. To avoid beam damage the sample was continuously scanned during the measurement at a carefully adjusted speed. The overall instrumental resolution was 140 meV in the case of the C 1*s*, 180 meV for the N 1*s*, and 280 meV for the Fe 2*p* photoemission line. All spectra were calibrated with respect to the Au 4*f* level of the sample at 83.96 eV (the multilayer thickness was chosen such that some Au 4*f* substrate signal was still visible). In essence, this way of calibration corresponds to calibrating to the substrate Fermi level. Since the FePc multilayer is characterized primarily by dispersion-type interactions the most appropriate energy reference would instead be the vacuum level,[31] the position of which we, however, could not determine at beam line I311 due to limitations of the experimental equipment. Finally, a polynomial-type background was subtracted from the Fe 2*p* and N 1*s* photoemission spectra, and from the C 1*s* spectra a Shirley-type background was subtracted.

For the least-square fit analysis performed on the N 1*s* and Fe 2*p* photoelectron spectra, a convolution of a Doniach–Šunjić and Gaussian line shapes was used for each component. For the symmetric peaks, where the Doniach–Šunjić asymmetry parameter is zero, the Doniach–Šunjić line shape reduces to a Lorentzian.

Supporting DFT calculations were performed employing the VASP package with the PBE-GGA (Perdew-Burke-Ernzerhof generalized gradient approximation) exchange-correlation potential. A plane-wave cutoff energy of 400 eV and spin polarization were used. Slab replicas were separated by 20 Å in the normal direction, leading to an effective vacuum region larger than 15 Å. The Brillouin zone was sampled with a single *k*-point at $\bar{\Gamma}$. To account for the multilayer conditions leading to a decoupling between the most of the FePc layers and the Au surface, a free FePc monolayer was considered in the calculations. The FePc and NH_3 molecules were allowed to relax until the self-consistent forces reached 20 meV/Å. In each electronic self-consistent step, an energy convergence of 10^{-3} meV was used.

III. RESULTS

Well-ordered multilayers of flat-lying FePc molecules were prepared by the procedure described above. The x-ray absorption spectra obtained on these multilayers (Fig. 2) show maximum intensity of the π^* resonances (resonances below ~405 eV) in grazing photon incidence. Their intensities decrease when going to less grazing incidence angles, and at normal incidence the intensity is quenched. The opposite angular behavior is observed for the σ^* shape resonances [resonances above ~405 eV and double peak feature at 399 eV (Ref. 32)]. The intensity variation of the XAS resonances with light incidence angle allows the exact determination of the molecular tilt angle with respect to the surface.[33] The inset in Fig. 2 displays the intensity variation of the lowest π^* resonance (LUMO) at around 398 eV, which is expected to change as[33]

$$A\,P\left(\cos^2(90^\circ-\vartheta)\,\cos^2\alpha+\frac{1}{2}\sin^2(90^\circ-\vartheta)\,\sin^2\alpha\right)$$

$$+A\,(1-P)\,\frac{1}{2}\sin^2\alpha,$$

where A is an amplitude, $P = 0.97$ is the degree of polarization of the beam line, ϑ is the light incidence angle, and α is the inclination of the normal of the isoindole molecular plane with respect to the surface normal. Fitting the data in the inset of Fig. 2 reveals that the normal of the molecular plane is oriented along the surface normal ($\alpha = 0^\circ$), proving a perfectly flat, ordered geometry of the multilayer FePc adsorbates.

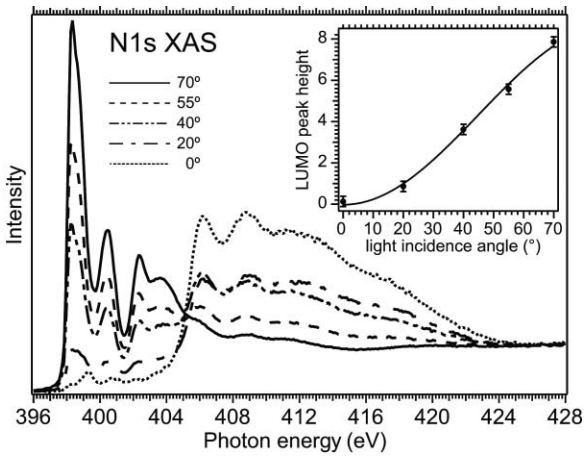

FIG. 2. Angle-resolved N 1*s* x-ray absorption spectra measured on a multilayer of FePc on Au(111); the inset shows the variation of the π^* LUMO resonance intensity as a function of light incidence angle with respect to the surface normal. The angular dependence proves a tilt angle of 0° of the LUMO with respect to the surface normal, showing thus a perfectly flat geometry of the multilayer FePc adsorbates.

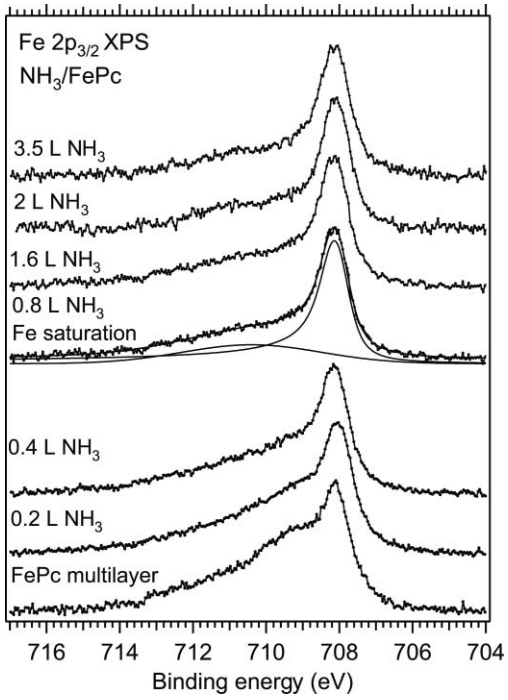

FIG. 3. Fe $2p_{3/2}$ x-ray photoelectron spectra. The bottom spectrum is the spectrum obtained on the clean FePc multilayer; the other spectra were measured after dosing NH_3. With increasing dose the spectra become significantly narrower, but no binding energy shift is observed. All spectra have been normalized to the height of the most intense component. The spectrum at saturation (0.8 L dose) shows both the experimental data and the result of the least-square fit. The results show two peak components, a main peak at 708.06 eV and a broad satellite peak at 710.38 eV. Least-square fits of the Fe $2p_{3/2}$ photoemission signal were performed using convolutions of Doniach–Šunjić and Gaussian line shapes for each component.

Increasing amounts (0.2 to 3.5 L) of NH_3 were dosed onto the multilayers held at ~20 K. The multilayer thickness was estimated to be of at least seven layers. The estimation was based on the relative intensity of the C 1*s* signal of the bottom layer of the FePc film [in direct contact with the Au(111) surface] with respect to the C 1*s* signal arising from the multilayer. The Fe $2p_{3/2}$ x-ray photoelectron spectra of the FePc multilayers before and after NH_3 adsorption are shown in Fig. 3. Prior to adsorption of NH_3 the Fe $2p_{3/2}$ signal is characterized by a broad line, the width of which is largely determined by the unpaired spins in the iron $3d^6$ valence states, which couple to the angular momentum of the core hole.[34–38] Upon NH_3 adsorption the shape of the Fe 2*p* signal starts to change gradually, becoming narrower with increasing amounts of gas. Once the NH_3 dose has reached 0.8 L, the Fe 2*p* peak shape remains unchanged even upon further NH_3 dosage. The drastic change of the line shape shows that NH_3 binds to all the iron ions of the FePc molecules in the multilayer, or at least to all FePc molecules which contribute to the photoemission signal. Hence, ammonia diffuses into the multilayer. The dose of 0.8 L corresponds to the point where all the Fe atoms probed in the photoemission experiment accommodate ammonia molecules, and in the following the corresponding NH_3 dose will be referred to as "saturation dose". It will be shown later from an analysis of the N 1*s* signal that the real saturation dose is actually slightly lower.

The bond between the FePc iron ion and the NH_3 adsorbate is expected to be a coordinate bond involving the lone pair orbital on the nitrogen atom and empty valence states on the FePc molecule. This coordinate bond is a relatively weak chemisorptive interaction. The relative weakness of the bond is reflected by the fact that the main component of the Fe 2*p* line at 708 eV is not shifted with respect to that measured on the multilayer even at saturation. The constant binding energy also indicates that the lone pair electrons are still highly localized on the NH_3 molecule. The decrease in FWHM of the Fe $2p_{3/2}$ line is very large--the FWHM is 3.7 eV before and 1.05 eV after adsorption of NH_3. This is larger than what would be expected for changes in the electronic structure and morphology of the FePc film. Instead, we will argue in the following that the narrowing of the Fe 2*p* photoemission line proves the formation of a low spin compound.

Basically, the broadening of the Fe $2p_{3/2}$ line shape is, to a large part, a consequence of a Zeeman-like splitting of the four m_j components (3/2, 1/2, −1/2, −3/2) in the magnetic field of the valence spin. m_j is the quantum number related to the *z*-component of the total angular momentum of the core hole. The higher the valence spin, the larger the split between the m_j components,[39] and in consequence the broader the spectrum. The changes in the FWHM of the Fe $2p_{3/2}$ photoemission line can thus be used as a measure for changes in the valence spin magnetic moment. The narrowing of the signal at saturation offers a clear indication of a significant decrease in the separation between the Fe $2p_{3/2}$ m_j components and thus in valence spin. This experimental interpretation is also supported by theoretical work. The ligand field created by the NH_3 molecules leads to a reorganization of the Fe 3*d* levels, which results in the pairing of the spins of the 6*d*-electrons. We have observed similar effects of quenching or reducing the spin state on the phthalocyanine metal center in the presence of different ligands in a previous study.[40] In more detail, from our own and from previously published work[28] it is known that, in the absence of any additional ligands, the energetic distribution of the iron 3*d* orbitals of FePc is characterized by the order $3d_{x^2-y^2} \gg 3d_{z^2} > 3d_{xy} \approx 3d_{xz,\,yz}$. Energetically, it is not favorable to place electrons inside the $3d_{x^2-y^2}$ states, and, thus, the application of Hund's rule implies that two of the six electrons will remain unpaired. In view of the geometric constraints, the ammonia lone pair is expected to interact primarily with the iron $3d_{z^2}$ orbital, leading to an upward energy shift. The $3d_{z^2}$ orbital becomes depopulated after NH_3 adsorption and instead the six *d* electrons completely fill the $3d_{xy}$, $3d_{xz}$, and $3d_{yz}$ orbitals. All spins are paired and the overall spin is quenched.

In Fig. 3 a least-square fit of the Fe $2p_{3/2}$ spectrum at saturation dose is shown. Table I shows the fit parameters. The spectrum contains a main peak at 708.06 eV with a FWHM of 1.02 eV and a broad satellite feature at 710.38 eV. The relatively low FWHM of the main peak matches well with the previous results of ours for low spin compounds formed by adsorption of NH_3 on monolayers of FePc on Au(111).[40,41] The lowering of the spin magnetic moment upon ammonia adsorption is also predicted by calculations: it is found to

TABLE I. Fe $2p_{3/2}$ peak parameters at saturation (0.8 L NH_3 dose). The LWHM (GWHM) is the Lorentzian (Gaussian) linewidth.

		BE (eV)	LWHM (eV)	Asymmetry parameter	GWHM (eV)	Area	FWHM
Multilayer + NH_3	Main peak	708.06	0.50	0.16	0.52	1.17	1.02
	Satellite	710.38	0	0	4.46	0.69	4.46

be $-0.27\ \mu_B$ after NH_3 adsorption, compared to $2.02\ \mu_B$ for free FePc.

Further information about the adsorption of NH_3 on FePc can be deduced from the evolution of the N 1*s* photoemission peaks with increasing NH_3 dose (cf. Fig. 4 for the spectra and Table II for some representative peak parameters). The N 1*s* photoemission signal from the FePc multilayer contains two features, a main peak (P1) at 398.57 eV and a low intensity shake-up satellite (P4) at 400.46 eV. A new component, labeled P3, appears when dosing the smallest amount (0.2 L) of NH_3. At this dose P3 has a binding energy of 399.85 eV. Upon an increase of the dose to 0.4 L P3 shifts to 399.75 eV and then remains constant in binding energy at higher ammonia doses (to within the uncertainty). Its area relative to that of the FePc N 1*s* signal increases up to the saturation dose [cf. Fig. 5(a)]. From that dose onward the P3 peak parameters remain unchanged, as do those of the Fe $2p_{3/2}$ line. This shows clearly that the P3 peak is due to NH_3 molecules bound to the Fe ions (Fe–NH_3 bonds). At saturation, the relative area of the P3 peak with respect to the FePc peak (P1) is 0.244, which from the stoichiometry of the FePc compound (eight nitrogen atoms) suggests that there are two ammonia molecules bound to each Fe center. This is in agreement with the fact that the valence band structure of the iron atom allows the formation of sixfold coordinated complexes, and it also agrees with the finding of diffusion of ammonia into the multilayer. In addition, DFT calculations performed on the gas phase FePc found an adsorption energy of -0.44 eV for the first NH_3 molecule, while for the second molecule the adsorption energy is -1.1 eV [see Fig. 6 for the structure of the $FePc(NH_3)_2$ complex], showing that indeed the formation of sixfold coordinated $FePc(NH_3)_2$ complexes is likely to take place.

In addition to P3 a new component P2 appears at the saturation dose at 399.41 eV. We assign it to additional NH_3 molecules adsorbed on FePc on other sites than the iron

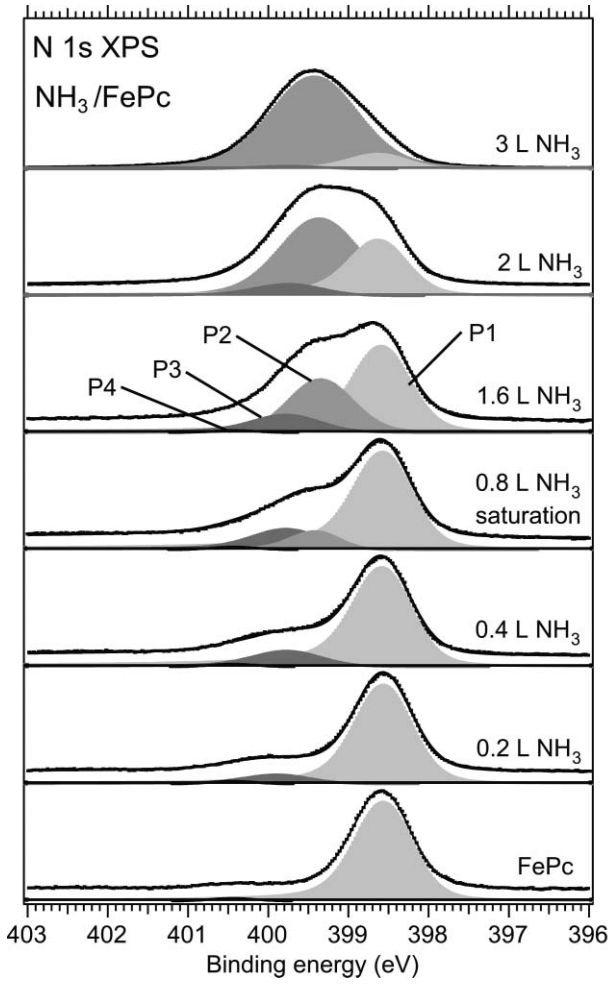

FIG. 4. Experimental data and fits of the N 1*s* x-ray photoelectron spectra before and after adsorption of NH_3 on multilayer FePc. The bottom spectrum is the spectrum of a clean FePc multilayer, characterized by the main peak (P1) and a shake-up satellite (P4). Ammonia adsorption results in additional peak components, P3 due to Fe–NH_3 bond formation and P2 due to NH_3 species adsorbed elsewhere on the macrocycle (Pc–NH_3 interactions). The spectra are normalized with respect to the height of the main peak.

TABLE II. N 1*s* peak parameters [binding energies (BE) and full widths at half maximum (FWHM) in eV, and relative areas with respect to the P1 main peak] for NH_3 doses up to 3.5 L on multilayer FePc/Au(111), as given by the results of the least-square fits. The BE and FWHM uncertainty is ±50 meV up to 1.6 L and ±100 meV at the high doses where the FePc signal starts to be attenuated.

Dose (L)	Peak parameter	N 1*s* peak			
		P1 (FePc)	P2 (NH_3)	P3 (Fe–NH_3)	P4 (Shake-up P1)
0 L	BE	398.57			400.46
(FePc multilayer)	FWHM	0.85			0.67
	Rel. area	1.00			0.02
0.2 L	BE	398.57		399.85	400.46
	FWHM	0.85		1.01	0.67
	Rel. area	1.00		0.11	0.02
0.4 L	BE	398.57		399.75	400.46
	FWHM	0.88		1.03	0.67
	Rel. area	1.00		0.18	0.02
0.8 L	BE	398.56	399.41	399.76	400.46
	FWHM	0.88	0.73	1.03	0.67
	Rel. area	1.00	0.15	0.244	0.02
1.6 L	BE	398.59	399.41	399.76	400.46
	FWHM	0.88	0.82	1.03	0.67
	Rel. area	1.00	0.43	0.244	0.02
2 L	BE	398.62	399.39	399.73	
	FWHM	0.88	1.17	1.03	
	Rel. area	1.00	1.71	0.243	
3.5 L	BE	398.62	399.44	399.73	
	FWHM	0.88	1.28	1.03	
	Rel. area	1.00	8.4	0.243	

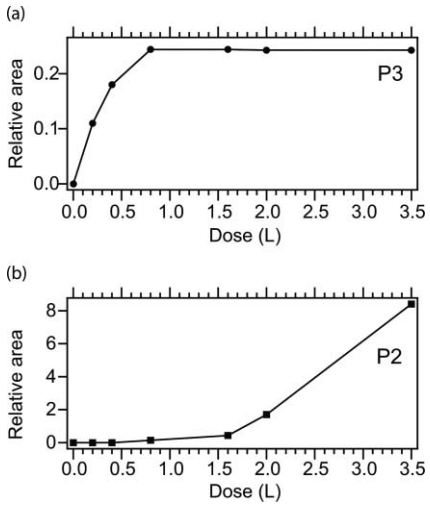

FIG. 5. Relative areas (with respect to the N 1*s* photoemission signal arising from the FePc molecules) of the N 1*s* P2 (a) and P3 (b) (Fe–NH_3) peaks.

(Pc–NH_3 interactions) as well as, at higher doses, NH_3 multilayer molecules. Since P2 is observed already at a dose of 0.8 L, it seems likely that the true saturation dose is somewhat lower. This would imply that all iron sites are occupied before adsorption occurs at any other site. This makes a very interesting difference to what we have observed for NH_3 adsorption on monolayers of FePc on Au(111) (Ref. 41): there simultaneous occupation of different sites is observed even for doses far below the saturation dose.

The notion that after saturation of the iron ions a first NH_3 layer is completed on top of the FePc film which then develops into a multilayer is supported by a consideration of the absolute intensities of the C 1*s* and N 1*s* spectra (not shown). Both the C 1*s* spectra and P1 and P3 components of the N 1*s* spectra start to be attenuated at a dose of 0.8 L, while the N 1*s* P2 component continues to grow [cf. Fig. 5(b)]. This also allows us to relate NH_3 dose and coverage: at around 0.8 L dose the first NH_3 layer is filled, i.e., a monolayer coverage is reached, not counting the ammonia molecules, though, which have diffused into the FePc film. The exact binding sites of this monolayer, other than the iron site, cannot be assigned more specifically, but we note that the binding energy and width of the P1 component of the N 1*s* spectra, i.e., of the component related to the FePc macrocycle, do not change (cf. Table II) and, likewise, that the C 1*s* spectra (not shown) remain the same for all doses. Hence, on the FePc macrocycle the ammonia molecules only physisorb. Since the C 1*s* and N 1*s* are attenuated in the same way at saturation dose, we also conclude that the physisorption is not specific to a particular site.

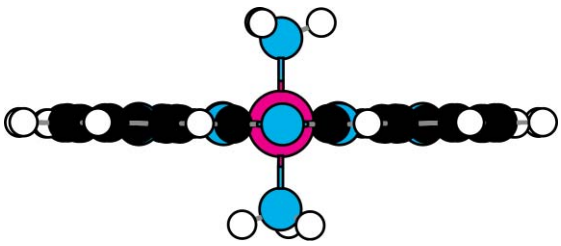

FIG. 6. Molecular structure of the $FePc(NH_3)_2$ complex.

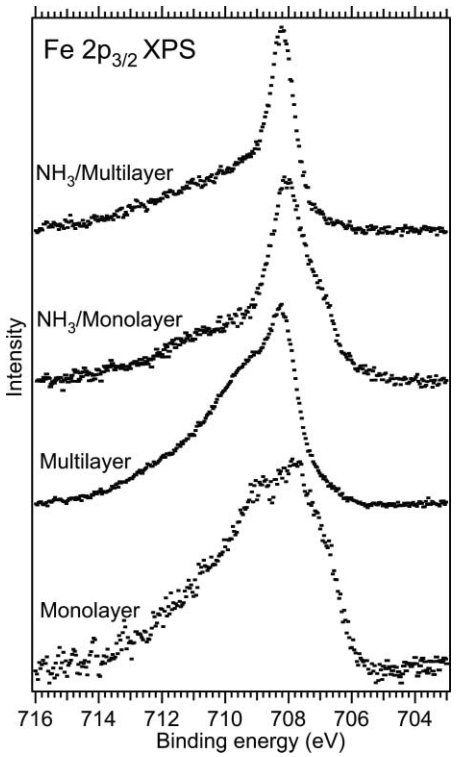

FIG. 7. Fe $2p_{3/2}$ photoemission lines for mono- and multilayers of FePc on Au(111) and the corresponding spectra after adsorbing NH_3 in amounts equal to the iron saturation dose. The monolayer spectra prior and after NH_3 adsorption show a low-binding energy shoulder which is caused by the interaction with the substrate and which is not present in the multilayer case. The spin of both mono- and multilayer is quenched after NH_3 adsorption.

One interesting aspect is a comparison between the present case of NH_3 adsorption on multilayer FePc/Au(111) and the adsorption of NH_3 on monolayer FePc/Au(111), reported by us previously.[41] Figure 7 shows the characteristic Fe $2p_{3/2}$ photoelectron spectra for mono- and multilayers of FePc on Au(111), as well as the corresponding spectra at saturation after NH_3 adsorption. For the Fe $2p_{3/2}$ photoemission line of monolayer FePc we found that, in addition to multiplet splitting effects, the line is broadened additionally by the interaction between the FePc adsorbates and the Au(111) substrate. The same holds after adsorption of NH_3. The interaction with the substrate is visible mainly through the low-binding energy shoulder at around 707 eV. The complete disappearance of this shoulder in the Fe $2p_{3/2}$ line of the multilayer FePc, both prior and after NH_3 adsorption nicely illustrates that no substrate influence is visible in the multilayer Fe 2*p* spectra. This basically shows that the relatively large FWHM of the Fe 2*p* multilayer line is mainly given by the unpaired spins in the valence band. The narrowing of the Fe 2*p* spectra after NH_3 adsorption is an indicator of the spin quench of the FePc molecule. Ammonia coordination to the Fe site produces similar effects on the spin state of both mono- and multilayer FePc.

The N 1*s* spectra at iron saturation also reveal some interesting differences between the adsorption behavior of NH_3 on multi- and monolayer of FePc on Au(111) (Fig. 8). First,

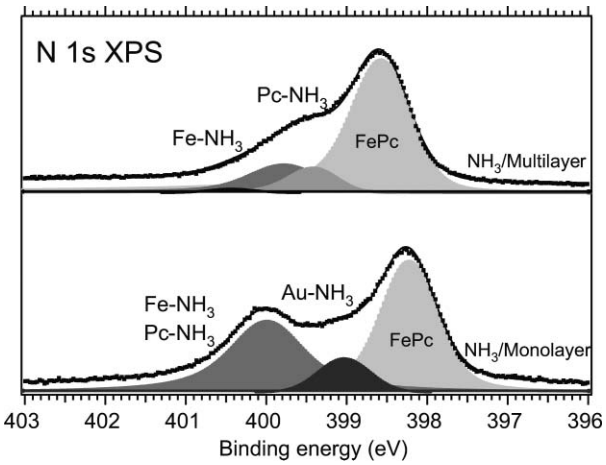

FIG. 8. N 1*s* photoemission spectra at saturation after NH_3 adsorption on monolayer FePc/Au(111) (bottom) and on multilayer FePc/Au(111) (top).

the adsorption on monolayer FePc results in a single peak at 400.01 eV for both the NH_3 species bound to iron and those adsorbed on the macrocycle (labeled Fe–NH_3 and Pc–NH_3 in Fig. 8). In constrast, the adsorption of NH_3 on the FePc multilayer results in two distinct peaks separated by around 0.35 eV (at 399.41 and 399.76 eV). The NH_3/monolayer adsorption also results in an additional peak due to Au(111)–NH_3 interactions. Second, as already discussed above, we find that NH_3 adsorption on FePc monolayers results in both the Fe–NH_3 and Pc–NH_3 species being present already at the initial doses of NH_3, while in the multilayer adsorption the Pc–NH_3 component appears only after all the iron sites are occupied. This shows that the Au(111) surface plays an important role in determining the ammonia adsorption behavior on FePc, possibly by lowering the adsorption energy for certain sites or by changing the diffusion behavior of the ammonia molecules.

IV. CONCLUSIONS

Adsorption of the electron donor species ammonia on multilayers of iron phthalocyanine supported by a Au(111) surface leads to significant changes of the electronic structure of the FePc molecular network. Most important, dative Fe–NH_3 bonds are formed, resulting in the formation of sixfold coordinated complexes. The formation of Fe–NH_3 bonds has a significant impact on the magnetic properties of the FePc molecule. The evolution of the Fe 2*p* photoemission spectra shape shows a transition from an open shell structure characteristic for the 3*d* valence band of the FePc to a closed shell, low-spin FePc$(NH_3)_2$ complex. The Fe–NH_3 interaction is rather weak, it does not result in any binding energy shift of the Fe 2*p* core levels. First all iron sites are occupied by ammonia, and only once saturation of the iron centers is reached adsorption on other sites starts to take place. This behavior is different from what we have observed in a previous study of adsorption of ammonia on monolayer FePc on Au(111), where several adsorption sites are populated already at the lowest doses of ammonia.

ACKNOWLEDGMENTS

The authors would like to acknowledge funding from the European Commission through the MONET Early Stage Researcher Training Network (Grant No. MEST-CT-2005-020908). Funding from Vetenskapsrådet (VR) is also acknowledged. We would like to thank the MAX-lab staff for technical support.

[1] L. R. Milgrom, *The Colours of Life: An Introduction to the Chemistry of Porphyrins and Related Compounds* (Oxford University Press, New York, 1997).
[2] N. B. McKeown, *Phthalocyanine Materials: Synthesis, Structure and Function* (Cambridge University Press, Cambridge, 1998).
[3] N. R. Armstrong, W. Wang, D. M. Alloway, D. Placencia, E. Ratcliff, and M. Brumbach, Macromol. Rapid Commun. **30**, 717 (2009).
[4] D. Hohnholz, S. Steinbrecher, and M. Hanack, J. Mol. Struct. **521**, 231 (2000).
[5] G. Gu, G. Parthasarathy, and S. R. Forrest, Appl. Phys. Lett. **74**, 305 (1999).
[6] C. D. Dimitrakopoulos and P. R. L. Malenfant, Adv. Mater. **14**, 99 (2002).
[7] G. de la Torre, C. G. Claessens, and T. Torres, Chem. Commun. (Cambridge) **20**, 2000 (2007).
[8] C. G. Claessens, U. Hahn, and T. Torres, Chem. Rec. **8**, 75 (2008).
[9] M. I. Newton, T. K. H. Starke, M. R Willis, and G. McHale, Sens. Actuators B **67**, 307 (2000).
[10] V. Vrkoslav, I. Jelinek, M. Matocha, V. Kral, and J. Dian, Mater. Sci. Eng., C **25**, 645 (2005).
[11] C. G. Claessens, W. J. Blau, M. Cook, M. Hanack, R. J. M. Nolte, T. Torres, and D. Wöhrle, Monatsch. Chem. **132**, 3 (2001).
[12] A. Palaniappan, S. Moochhala, F. E. H. Tay, X. Su, and N. C. L. Phua, Sens. Actuators B **129**, 184 (2008).
[13] S. Maldonado, E. Garcia-Berrios, M. D. Woodka, B. S. Brunschwig, and N. S. Lewis, Sens. Actuators B **134**, 521 (2008).
[14] A. M. Paoletti, G. Pennesi, G. Rossi, A. Generosi, B. Paci, and V. R. Albertini, Sensors **9**, 5277 (2009).
[15] M. Dubey, S. L. Bernasek, and S. Schwartz, J. Am. Chem. Soc. **129**, 6980 (2007).
[16] S. Singh, S. K. Tripathi, and G. S. S. Saini, Mater. Chem. Phys. **112**, 793 (2008).
[17] X. Ma, H. Chen, M. Shi, G. Wu, M. Wang, and J. Huang, Thin Solid Films **489**, 257 (2005).
[18] O. L. Kaliya, E. A. Lukyanets, and G. N. Vorozhtsov, J. Porphyr. Phthalocyanines **3**, 592 (1999).
[19] J. C. Obirai and T. Nyokong, J. Electroanal. Chem. **600**, 251 (2007).
[20] Y. Lu and R. G. Reddy, Int. J. Hydrogen Energy **33**, 3930 (2008).
[21] M. Toledo, A. M. S. Lucho, and Y. Gushikem, J. Mater. Sci. **39**, 6851 (2004).
[22] C. G. Claessens, U. Hahn, and T. Torres, Chem. Rec. **8**, 75 (2008).
[23] Z. Li, B. Li, J. Yang, and J. G. Hou, Acc. Chem. Res. **43**, 954 (2010).
[24] N. Tsukahara, K. Noto, M. Ohara, S. Shiraki, N. Takagi, Y. Takata, J. Miyawaki, M. Taguchi, A. Chainani, S. Shin, and M. Kawai, Phys. Rev. Lett. **102**, 167203 (2009).
[25] Z. Hu, B. Li, A. Zhao, J. Yang, and J. G. Hou, J. Phys. Chem. C **112**, 13650 (2008).
[26] M. S. Liao and S. Schneier, J. Chem. Phys. **114**, 9780 (2001).
[27] M. Grobosch, V. Y. Aristov, O. V. Molodtsova, C. Schmidt, B. P. Doyle, S. Nannarone, and M. Knupfer, J. Phys. Chem. C **113**, 13219 (2009).
[28] X. Lu and K. W. Hipps, J. Phys. Chem. C **101**, 5391 (1997).
[29] R. Nyholm, J. N. Andersen, U. Johansson, B. N. Jensen, and I. Lindau, Nucl. Instrum. Methods Phys. Res. A **467–468**, 520 (2001).
[30] J. Schnadt, J. Schiessling, J. N. O'Shea, S. M. Gray, L. Patthey, M. K. J. Johansson, M. Shi, J. Krempasky, J. Åhlund, P. G. Karlsson, P. Persson, N. Mårtensson, and P. A. Brühwiler, Surf. Sci. **540**, 39 (2003).
[31] T. C. Chiang, G. Kaindl, and T. Mandel, Phys. Rev. B **33**, 695 (1986).
[32] J. Åhlund, K. Nilson, J. Schiessling, L. Kjeldgaard, S. Berner, N. Mårtensson, C. Puglia, B. Brena, M. Nyberg, and Y. Luo, J. Chem. Phys. **125**, 034709 (2006).
[33] J. Stöhr, *NEXAFS Spectroscopy* (Springer-Verlag, Berlin Heidelberg, 1992).
[34] J. Weissenrieder, M. Göthelid, M. Månsson, H. von Schenck, O. Tjernberg, and U. O. Karlsson, Surf. Sci. **527**, 163 (2003).

[35]F. Sirotti and G. Rossi, Phys. Rev. B **49**, 15682 (1994).
[36]F. Sirotti, M. D. Santis, and G. Rossi, Phys. Rev. B **48**, 8299 (1993).
[37]C. Bethke, E. Kisker, N. B. Weber and F. U. Hillebrecht, Phys. Rev. B **71**, 024413 (2005).
[38]C. S. Fadley and D. A. Shirley, Phys. Rev. A **2**, 1109 (1970).
[39]G. van der Laan, Phys. Rev. B **51**, 240 (1995).
[40]C. Isvoranu, B. Wang, K. Schulte, E. Ataman, J. Knudsen, J. N. Andersen, M. L. Bocquet, and J. Schnadt, J. Phys.: Condens. Matter **22**, 472002 (2010).
[41]C. Isvoranu, B. Wang, E. Ataman, K. Schulte, J. Knudsen, J. N. Andersen, M. L. Bocquest, and J. Schnadt J. Chem. Phys. **134**, 114710 (2011).